



**NANYANG TECHNOLOGICAL UNIVERSITY
RENAISSANCE ENGINEERING PROGRAMME**

RE1013 – MATERIALS & MANUFACTURING MID-TERM PAPER

Lab Tests and Countermeasures to defeat the Tay-minator

Team Members: Huang Jing

 Jayanth Ramkumar

 Siah Zi En

 Wai Yan Aung

 Yang Xianyan, Winston

 Yuen Li Ying

TBL Group No.: TBL 8

Date of Submission: 31 October 2025

Table of Contents

1. Introduction	3
2. Differentiating Tests.....	3
2.1 Compositional and Microstructural Features via EDX and SEM.....	3
2.2 Magnetism Test.....	4
2.3 Tensile Strength Test.....	5
2.4 Chemical Reactivity Test	6
2.5 Permeability to Ionising Radiation Test.....	7
3. Justification	7
4. Appendix	9
5. References	12

Scope of Work

Huang Jing	1, Decision tree, 3
Jayanth Ramkumar	2.1, 3
Siah Zi En	2.4, 3
Wai Yan Aung	2.5, 3
Yang Xianyan, Winston	2.3, 3
Yuen Li Ying	2.2, 3

1. Introduction

The shards recovered from the first Tay-minator present a rare chance to uncover its material weaknesses. As outlined in Figure 1, the investigation follows a stepwise approach, from microstructural and magnetic analysis to mechanical and chemical testing, to identify the shard's composition, strength, and reactivity. Each stage guides the selection of the most effective destruction method, as well as the ease of implementing the countermeasure.

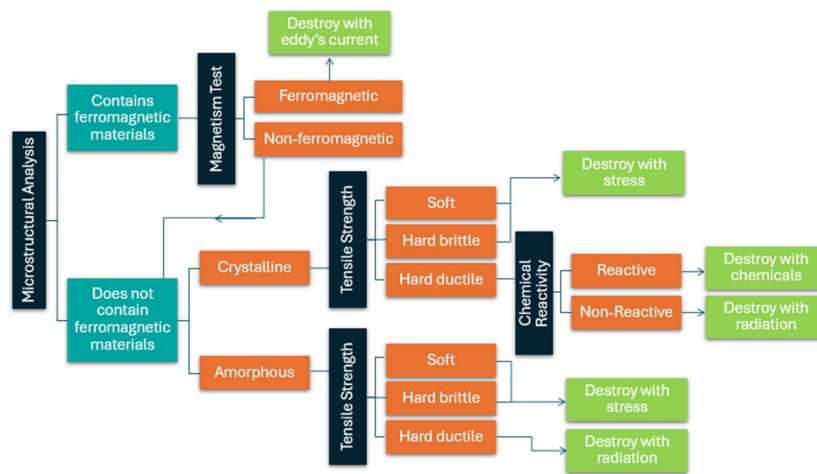


Figure 1: Experimental Flowchart

2. Differentiating Tests

2.1 Compositional and Microstructural Features via EDX and SEM

Microstructural analysis reveals whether the shard is crystalline or amorphous, while compositional analysis determines what elements are present within the sample. For sample preparation, mechanical polishing will be done using fine diamond or silicon carbide. However, if the material is too hard, Broad Ion Beam (BIB) polishing could be done instead [1]. This will create a smooth surface free of mechanical stress.

First, Energy-Dispersive X-ray Spectroscopy (EDX) is performed in the Scanning Electron Microscope (SEM) [2]. This provides the elemental composition to identify the metals and alloying composition and see if there are any ferromagnetic elements involved. (Appendix 1).

Once the material is identified, chemical etching can be carried out using alloy-specific etchants. This helps create contrast to identify features such as grain boundaries. The sample will then be observed under the SEM, which will allow us to observe microstructural features.

The presence of grain boundaries suggests a crystalline structure. The density of the grain boundaries influences the mechanical properties. According to the Hall-Petch relationship $\sigma = \sigma_0 + kd^{-\frac{1}{2}}$, the strength increases as the average grain size decreases, since grain boundaries act as barriers to dislocation motion, but ductility decreases. In addition, atoms at the boundaries also have high surface energy and are primary initiation sites for chemical reactions, increasing vulnerability to corrosion or chemical attacks. Conversely, the lack of grain boundaries indicates the metal is amorphous. This renders chemical countermeasures a less effective and time-consuming effort; thus, chemical attack is not recommended [3].

2.2 Magnetism Test

The magnetic-response test determines whether the shard, if it contains ferromagnetic metal, is actually ferromagnetic, verifying if the material's structure supports magnetic coupling for efficient energy transfer.

A strong neodymium magnet and a Hall probe are used to test for attraction and surface residual magnetic flux density. If coatings are present, the material can be polished in the same manner as above before testing. For quantitative results, vibrating-sample magnetometry (VSM) is used to obtain an M-H (magnetisation vs magnetic field) curve (Appendix 2) which determines key parameters such as saturation magnetisation (A, D), retentivity (B, E) and coercivity (C, F) [4].

A M–H hysteresis loop with non-zero retentivity and finite coercivity shows ferromagnetism. In such materials, repeated magnetisation cycling produces hysteresis heating, where energy dissipates as heat proportional to the loop area and excitation frequency, raising local temperature and driving microstructural changes such as precipitate softening or accelerated oxidation to destroy the shard. Follow-up electromagnetic characterisation, such as frequency-dependent permeability, loss factor, and skin-depth measurements, can quantify how efficiently magnetic energy is converted into local thermal and mechanical stress for destruction.

If only weak attraction and a linear M–H response are observed, the material is non-ferromagnetic. This suggests electromagnetic coupling is poor; hence, testing should continue along structural and chemical analysis to identify alternative vulnerabilities.

2.3 Tensile Strength Test

For non-ferromagnetic materials, we will test tensile strength, the maximum stress a material can withstand before failure under tension [5], corresponding to the Ultimate Tensile Strength (UTS) σ_{UTS} on the stress-strain curve. Brittle materials reach UTS and quickly fracture with minimal plastic deformation, while ductile materials deform plastically before failure [5].

Sufficiently soft and ductile materials can be machined down to obtain sub-size dog-bone specimens for tensile testing. Harder materials can be prepared using Electrical Discharge Milling (EDM), which erodes the hard conducting materials without inducing significant mechanical stress or heat-affected zones [6].

A universal testing machine will be used to determine the elasticity, yield strength, and elongation at fracture from stress-strain data. For EDM-prepared samples, a surrogate method (instrumented micro-indentation or small-punch testing) can be used to estimate tensile behaviour [7]. The resulting indentation depth and recovery profile are recorded to determine the hardness (H) and elastic-plastic response of the surface. Hardness and tensile strength are

both governed by a material's resistance to plastic deformation; empirical correlations can be used to approximate tensile strength from hardness values (for metals, a common relationship is $\sigma_{UTS} \approx 3 \times H$) [8]. A brittle material can be fractured by a high-velocity kinetic impact, while a more ductile or elastic material with higher σ_{UTS} would suggest that mechanical defeat is not as practical.

Commented [#YA1]: Add example of a most effective kinetic attack?

2.4 Chemical Reactivity | Test

For hard and ductile crystalline materials, the chemical reactivity will be determined by testing its resistance to corrosion, defined as a metal's ability to withstand deterioration due to corrosion [5]. Assuming the material is highly unreactive at room temperature, an acid immersion test is conducted to test the corrosion resistance under accelerated conditions and hence assess the structural integrity.

Commented [#LY2]: Cite appendix figure 3 somewhere in the paragraph

Concentrated Sulfuric Acid (H_2SO_4 , 98%) is prepared in a chemical fume hood using reagent grade acid and distilled water. To remove coatings, the shard is cleaned with acetone and distilled water and weighed to establish initial mass. It is then immersed in acid for 24 hours at an elevated temperature ($107^\circ C$) to increase rate of corrosion [6]. Once, done the shard is rinsed thoroughly with distilled water to prevent further corrosion, and the shard is re-weighed.

The corrosion rate can be calculated by (Corrosion Rate (mm/year) = (mass loss \times 87,600) / (surface area \times time \times metal density) which determines the material's vulnerability to concentrated chemical attack. Corrosion deteriorates physical conditions of the sample, leading to decreased tensile strength and hardness [11]; a highly corroded sample suggests that a hybrid approach by using concentrated acids and kinetic impact could be effective in overcoming the material.

2.5 Permeability to Ionising Radiation Test

The final test assesses the shard's permeability to ionising radiation. This requires sophisticated equipment, and the countermeasure is challenging to execute; hence is considered a last-resort option for hard, ductile amorphous or non-reactive, hard-ductile and crystalline metals.

The penetration power of ionising radiation is based on how likely they are to interact with the matter they are passing through and their energy levels (Appendix 4). Metals with lower atomic number and density also have higher penetrability (Appendix 4). We will test for gamma rays and neutrons, the two ionising radiations with the highest penetration powers [12], using a gamma ray source, a neutron source, and a scintillation detector that can detect both (Appendix 4). The counts recorded with and without the shards using a scintillator will indicate the shielding effectiveness. If the shard is permeable to both gamma rays and neutrons, high-energy linear accelerators (LINACs) can serve as a countermeasure [13]. This delivers megavoltage X-ray beams with high energy and properties identical to gamma rays [14], while simultaneously, linacs produce photoneutrons [15]. If only neutron permeability is observed, a deuterium-tritium fusion neutron generator can be focused into a neutron beam using a collimator that allows only parallel streams to pass through, creating a concentrated beam [16].

3. Justification

Performing the EDX first is crucial as it provides us the elemental composition of the shards, giving us a rough idea what we are dealing with. Microstructural analysis is carried out immediately after, as EDX uses the SEM. This allows us to analyse the grain boundaries. However, this is simply a diagnostic test, not a countermeasure. If the EDX reveals ferromagnetic materials such as Fe, Co and Ni, we will conduct the magnetism test, since ferromagnetic behaviour is only exhibited in certain compositions in alloys. Eddy current heating can then be used to overcome the material if it is ferromagnetic.

If no ferromagnetic material is found, subsequent tests are used to narrow down the weakness of the material. The selection of subsequent tests was based on conditions of the thermonuclear blast, which produced an environment characterised by kinetic impact, high temperature, and ionising radiation.

We first proceed to the tensile strength test. The grain boundary density in crystalline solids is closely related to the strength of the material, hence making tensile strength the logical next step. In addition, the tensile strength test is quicker to conduct than chemical reactivity. As amorphous materials are chemically inert, the tensile strength test is also essential in determining our future approach. If the material is soft or hard and brittle, a kinetic impact approach would be preferred as the most feasible and viable solution, given the immediate availability of weapons.

If the material has a crystalline microstructure and is hard and ductile, chemical reactivity will be tested since the presence of grain boundaries increases chemical reactivity; if reactive, corrosion can be induced to reduce the UTS, after which we can use high-velocity impact.

For chemically inert hard and ductile materials, we test for permeability to ionising radiation as a last resort. Upon penetration, ionizing radiation can damage internal circuitry by knocking electrons and physically displacing atoms in semiconductors, and cause single-event effects (SEE) that can cause immediate component damage [17] [18]. We assume that the Terminator's internal electronics use standard semiconductors that are vulnerable to these attacks.

A table of the possible materials for each given condition and test has been included in Appendix 3. |

Commented [#R3]: for hard, ductile and reactive use copper:

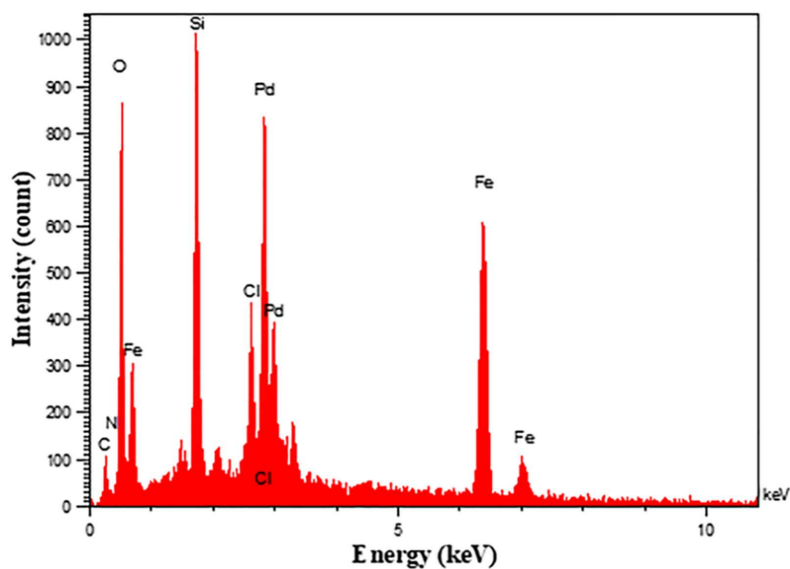
<https://fractory.com/copper-corrosion/>

<https://academy.ampcometal.com/copper-based-alloys-relationship-between-ductility-and-strength>

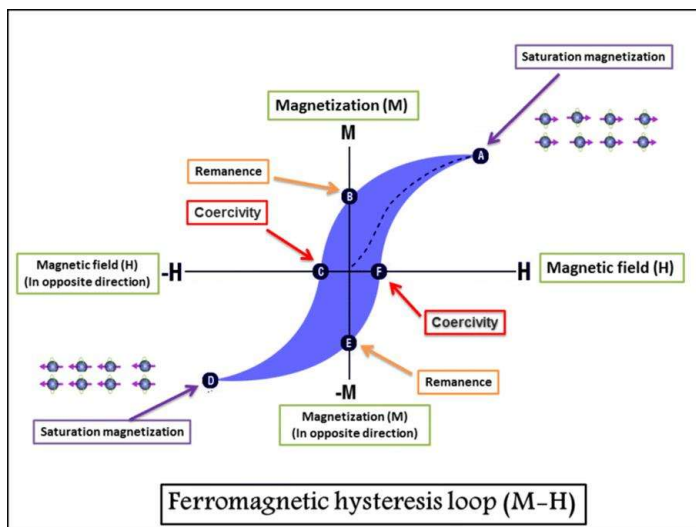
Commented [#R4R3]: Mg-Zn-Ca BMG with rare earth Y for amorphous soft

<https://www.intechopen.com/chapters/86381>

4. Appendix



Appendix 1: EDX Diagram (Karimi et. al, 2023) [24]



Appendix 2: Ferromagnetic hysteresis loop (M-H curve) [4]

Ferromagnetic	Non-ferromagnetic						
	Crystalline				Amorphous		
	Soft	Hard, Brittle	Hard, Ductile		Soft	Hard, Brittle	Hard, Ductile
Examples:	Examples:	Examples:	<u>Reactive</u>	<u>Non-reactive</u>	Examples:	Examples:	Examples:
- Iron	- Aluminium [19]	- Nickel Aluminide (NiAl) [20]	Examples: - Copper based alloys [21] [22]	Examples: - Austenitic stainless steels	- Mg-Zn-Ca BMG with rare earth Y [23]	- Zirconium-based amorphous alloys	- Yttrium-doped Zr-based BMGs [25]
- Nickel	- Group I metals			- Ni-Cr-Mo alloys		- Titanium-based amorphous alloys [24]	- Zr-based BMGs with Nanoscale Inhomogeneity [26]
- Cobalt							
- Some steels (carbon steel ferritic and martensitic stainless steels)							

Appendix 3: Table of Possible Materials

Appendix 4: Permeability of Ionising Radiation

Different ionising radiations have different levels of permeability based on how likely they are to interact with the matter they are passing through and their energy levels. As electromagnetic waves, X-rays and gamma rays have high penetration power since they are uncharged and don't interact as frequently with the electrons of the matter they pass through. Gamma rays have higher penetration power as they have a higher frequency and hence higher energy [27]. Neutrons have the highest penetration power as although they may have different energy levels based on the neutron source. They are electrically neutral, so they do not interact with the electron clouds of atoms and only interact with atomic nuclei, which is less frequent, allowing them to travel further before colliding [28]. Different metals also have different permeability to ionising radiation. Metals with lower atomic numbers have fewer subatomic particles, such as protons and electrons, and a smaller atomic size, reducing the chances of radiation interacting with an atom and losing energy [29].

As for measuring the ionising radiation permeability of the shards to gamma rays and neutrons, we can use scintillation detectors. Scintillators are a type of material that releases a flash of light when exposed to ionising radiation, which is then detected and amplified by a photomultiplier tube, which is then measured by the detector [30]. There are commercially available scintillators that are responsive to both gamma rays and neutrons, and even able to do so simultaneously [31]. The gamma rays can come from radioactive sources, such as ^{137}Cs [32], while the neutrons can come from fusion neutron generators, such as deuterium-deuterium or deuterium-tritium fusion neutron generators [16]. LINACs may even be possible sources of both gamma rays and neutrons, although it is less controlled [33].

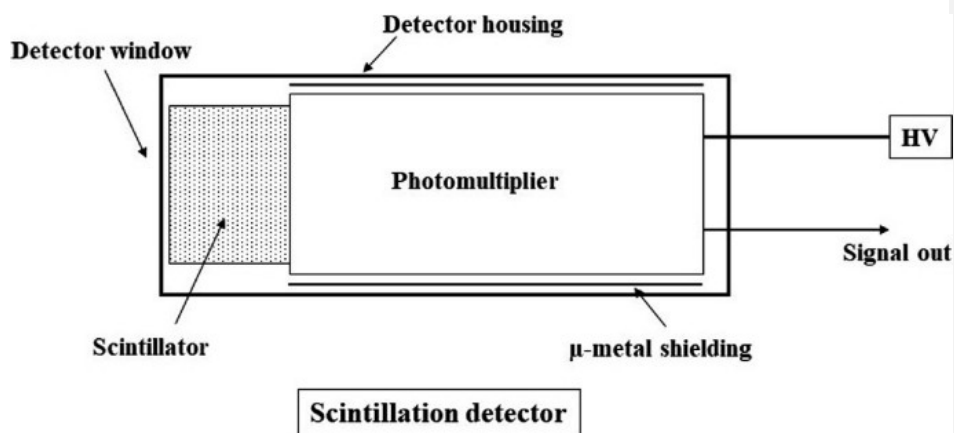


Figure 2: Diagram of a scintillation detector [34]

5. References

- [1] Nanoscience Instruments. (2025). *Broad Ion Beam vs. Focused Ion Beam Polishing: Choosing the Right Technique for Sample Preparation*. Retrieved from nanoScience Instruments: <https://www.nanoscience.com/blogs/broad-ion-beam-vs-focused-ion-beam-polishing-choosing-the-right-technique-for-sample-preparation/>
- [2] Antonis Nanakoudis. (2019, November 28). *EDS Analysis with SEM: How Does it Work?* Advancing Materials; ThermoFisher Scientific. <https://www.thermofisher.com/blog/materials/ed-analysis-with-sem-how-does-it-work/>
- [3] Lynne. (2007). *Amorphous Solid*. Retrieved from Science Direct: <https://www.sciencedirect.com/topics/engineering/amorphous-solid>
- [4] Yakout. (2020). Retrieved from https://www.researchgate.net/figure/Ferromagnetic-hysteresis-loop-M-H-curve-observed-in-the-ferromagnetic-materials_fig13_341780478
- [5] Callister & Rethwisch. (2018). *Material Science and Engineering: An Introduction*. Retrieved from [https://ftp.idu.ac.id/wp-content/uploads/ebook/tdg/TEKNOLOGI%20REKAYASA%20MATERIAL%20PERTAHANAN/Materials%20Science%20and%20Engineering%20An%20Introduction%20by%20William%20D.%20Callister,%20Jr.,%20David%20G.%20Rethwisch%20\(z-lib.org\).pdf](https://ftp.idu.ac.id/wp-content/uploads/ebook/tdg/TEKNOLOGI%20REKAYASA%20MATERIAL%20PERTAHANAN/Materials%20Science%20and%20Engineering%20An%20Introduction%20by%20William%20D.%20Callister,%20Jr.,%20David%20G.%20Rethwisch%20(z-lib.org).pdf)
- [6] Qudeiri. (2020, March 19). *Principles and Characteristics of Different EDM Processes in Machining Tool and Die Steels*. Retrieved from MDPI: <https://www.mdpi.com/2076-3417/10/6/2082>
- [7] Lucon. (2020, June). *Small Punch Testing to Estimate Mechanical Properties of Additively Manufactured Ti-6Al-4V*. Retrieved from <https://nvlpubs.nist.gov/nistpubs/TechnicalNotes/NIST.TN.2096.pdf>
- [8] Pavlina, & Tyne. (2008, February 1). *Correlation of Yield Strength and Tensile Strength*. Retrieved from <https://wpfiles.mines.edu/wp-content/uploads/aspprc/ResearchMaterials/Publications/386-Pavlina.pdf>

- [9] AMPCO. (2025). *Corrosion Resistance*. Retrieved from <https://www.ampcometal.com/applications/corrosion-resistance/>
- [10] Panossian. (2009). *CORROSION BY CONCENTRATED SULFURIC ACID IN*. Retrieved from <https://www.osti.gov/etdeweb/servlets/purl/21319914>
- [11] Hou. (2016). *Experimental Investigation on Corrosion Effect on*. Retrieved from <https://vuir.vu.edu.au/34591/1/5808372.pdf>
- [12] Auvinen. (2000). *Ionizing Radiation, Part 1: X- and Gamma (γ)-Radiation, and Neutrons*. Retrieved from National Library of Medicine: <https://www.ncbi.nlm.nih.gov/books/NBK401325/>
- [13] Suliman. (2023). *Photoneutrons and Gamma Capture Dose Rates at the Maze Entrance of Varian TrueBeam and Elekta Versa HD Medical Linear Accelerators*. Retrieved from PubMed Central: <https://pmc.ncbi.nlm.nih.gov/articles/PMC9867262/>
- [14] Hossein, & Ali. (2025). *Megavoltage Radiation*. Retrieved from Science Direct: <https://www.sciencedirect.com/topics/biochemistry-genetics-and-molecular-biology/megavoltage-radiation#definition>
- [15] Khilafath. (2022). *Evaluation of photoneutron dose equivalent in 10 MV and 15 MV beams for wedge and open fields in the Elekta Versa HD linac*. Retrieved from Science Direct: <https://www.sciencedirect.com/science/article/abs/pii/S0969804322002524>
- [16] SHINE. (2025). *What is a Neutron Beam?* Retrieved from SHINE Technologies: <https://www.shinefusion.com/blog/what-is-a-neutron-beam>
- [17] Colby. (2025). *Radiation Hardening Techniques for Spacecraft Electronics PCB: A Comprehensive Guide*. Retrieved from AllElectroHub: <https://www.allpcb.com/blog/pcb-knowledge/radiation-hardening-techniques-for-spacecraft-electronics-pcb-a-comprehensive-guide.html>

- [18] LaFond. (2025). *Cosmic Ray Bit Flips and the Hidden Risk at Scale*. Retrieved from <https://cside.com/blog/cosmic-ray-bit-flips-and-the-hidden-risk-at-scale>
- [19] AZOMaterials. (2005). *Aluminium: Specifications, Properties, Classifications and Classes*. Retrieved from <https://www.azom.com/article.aspx?ArticleID=2863>
- [20] Sampath. (2023). *An Overview on Synthesis, Processing and Applications of Nickel Aluminides: From Fundamentals to Current Prospects*. Retrieved from MDPI: <https://www.mdpi.com/2073-4352/13/3/435>
- [21] Sild. (2024). *Copper Corrosion Explained*. Retrieved from <https://fractory.com/copper-corrosion/>
- [22] AMPCO. (2021). *Copper based alloys: Relationship between ductility and strength*. Retrieved from <https://academy.ampcometal.com/copper-based-alloys-relationship-between-ductility-and-strength>
- [23] Li, & Xie. (2023). *Development of Mg-Based Bulk Metallic Glasses and Applications in Biomedical Field*. Retrieved from <https://www.intechopen.com/chapters/86381>
- [24] Hales. (2020). *Hardness-Strength Correlations in Zr(Cu)-Based*. Retrieved from <https://ntrs.nasa.gov/api/citations/20205007062/downloads/NASA-TP-2020-5007062Final.pdf>
- [25] Fu. (2025). *Industrial applicable, Be-Ni-free Y-doped Zr-based bulk metallic glasses with high glass-forming ability and superior mechanical properties*. Retrieved from <https://www.sciencedirect.com/science/article/pii/S0925838825022212>

- [26] Cheng. (2019). *Ductile Zr-Based Bulk Metallic Glasses by Controlling Heterogeneous Microstructure from Phase Competition Strategy*. Retrieved from <https://www.mdpi.com/2079-4991/9/12/1728>
- [27] Gordon. (n.d.). *Penetrating Power of Radiation*. Retrieved from [https://chem.libretexts.org/Bookshelves/Introductory_Chemistry/Chemistry_for_Changing_Times_\(Hill_and_McCreary\)/11:_Nuclear_Chemistry/11.06:_Penetrating_Power_of_Radiation](https://chem.libretexts.org/Bookshelves/Introductory_Chemistry/Chemistry_for_Changing_Times_(Hill_and_McCreary)/11:_Nuclear_Chemistry/11.06:_Penetrating_Power_of_Radiation)
- [28] Ossila. (2025). *Neutron Radiation, Emission and Scattering*. Retrieved from <https://www.ossila.com/pages/neutron-radiation>
- [29] Paek. (2025). *What Blocks Radiation? Materials Used in Radiation Shielding*. Retrieved from <https://www.lancsindustries.com/blog/materials-used-radiation-shielding/>
- [30] Hilger Crystals. (2023). *How Do Scintillators Work?* Retrieved from <https://www.hilger-crystals.co.uk/2023/04/13/how-do-scintillators-work/>
- [31] BNC. (2025). *CLYC:Ce Gamma / Neutron Scintillators*. Retrieved from Berkeley Nucleonics Corp : <https://www.berkeleynucleonics.com/clycce/>
- [32] Najam. (2014). *Science and Education Publishing*. Retrieved from <https://pubs.sciepub.com/ijp/2/1/5/>
- [33] Lin. (2014). *Development of high-sensitivity neutron detectors and measurements at the TPS LINAC* . Retrieved from https://www.aesj.net/document/pnst004/648_652.pdf
- [34] Leon. (2022). *Scintillation Detectors*. Retrieved from https://link.springer.com/chapter/10.1007/978-3-031-09970-0_10